Materials Research. 2021; 24(5): e20200487
DOI: https://doi.org/10.1590/1980-5373-MR-2020-0487

Microstrip Patch Antenna with $BiNbO_4(V_2O_5)$ Substrate and Copper Periodic Structures

Igor Ramon Sinimbú Miranda[a,b]*, ***Fiterlinge Martins de Sousa***[a], ***Fabio Barros de Sousa***[a], ***Jorge Everaldo de Oliveira***[c], ***Marcos Benedito Caldas Costa***[a,b]

[a]*Universidade Federal do Pará, Programa de Pós-Graduação em Engenharia Elétrica (PPGEE), Belém, PA, Brasil.*
[b]*Universidade Federal do Pará, Faculdade de Física (FACFIS/CANAN), Ananindeua, PA, Brasil.*
[c]*Universidade Federal do Sul e Sudeste do Pará (UNIFESSPA), Instituto de Ciências Exatas (ICE), Marabá, PA, Brasil.*

Received: October 21, 2020; Revised: March 08, 2021; Accepted: July 12, 2021

The use of high permittivity materials on substrates of a microstrip antenna was developed with Bismuth Niobate ceramic doped with vanadium Oxide ($BiNbO_4$ (V_2O_5)) and compared with an antenna of silicon dioxide substrate (SiO_2) using Ansys software HFSS and CST Studio. The ceramic antenna has -20 dB at 3.5 GHz and the silicon dioxide antenna -24.7 dB of reflection coefficient. The bandwidth values are 80 MHz for the bismuth ceramic antenna and 100 MHz for the silica antenna. The results demonstrate that the proposed $BiNbO_4$ antenna has great advantage compared to those mentioned in terms of volume reduction, presenting results similar to those antennas with higher volume. In addition, we use copper periodic structures (EBG) in order to increase the gain in associated with the use of $BiNbO_4$ with addition of V_2O_5 on the antenna substrate leading to a reduction in the total volume. Therefore, the proposed Bismuth Niobate antenna proves to be an excellent alternative for 5G technology and microwave S band (2-4 GHz) devices, highlighting the mentioned advantages.

Keywords: *Bismuth Niobate Ceramic, 5G technology, Microstrip Antenna.*

1. Introduction

The Fifth Generation of Mobile Communication System(5G) emerged due to the need of solving the problems of High data rate, low latency and the explosive growth in mobile data traffic[1,2]. Besides that, frequency bands have been established and specified by the International Telecommunication Union (ITU) defined to the fifth generation (5G) mobile communication system (IMT-2020)[2]. In this perspective the S band (2GHz to 4GHz) highlights for mobile communications, specifically the 3.5GHz frequency band[2].

Within this, the use of electroceramic materials in antennas appears as a viable option for presenting high dielectric constants and loss reduction in addition of low magnetic impurities, which leads to a small level of non-linearities in the material (intermodulation)[3]. Ceramic materials with $\varepsilon_r > 20$ are commonly used in miniaturization of antennas, enabling the insertion of these elements in portable devices[4,5]. To characterize these materials and their possible applications in mobile communication devices, for example, some properties that describe dielectric materials are important such as: the quality factor (Q), the dielectric constant (ε_r) and the temperature coefficient at the resonance frequency (τ_f)[3].

Over the years, ceramic materials have been widely used in microwave devices such as: antennas, filters and frequency selective surfaces (FSS). Cheng-Fu Yang[6] studied the sintering characteristics of $BiNbO_4$ with different amounts of CuO, V_2O_5 or CuO-V_2O_5 mixtures obtaining high quality values by adding CuO-V_2O_5 as sintering aids and shifting the temperatures values. In 2000, Tzou et al.[7] investigated the microwave dielectric properties of $BiNbO_4$ as function of the addition of V_2O_5, their optimum value of microwave properties were: $\varepsilon_r = 43.6$, $\tau_f = +13.8$ ppm/ºC and $Q = 3410$.

Shihua et al.[8] also investigated the microwave properties of $BiNbO_4$ doped with B_2O_3 this time. The optimum values of dielectric constant, Q-value and TCF-value at 4.8 GHz were 41.5, 4400 and −2.4 ppm/◦C, respectively. Zhou et al.[9] developed a two elements microstrip antenna with $BiNbO_4(V_2O_5)$ substrate to operate in 3.5 GHz obtaining 50 MHz of bandwidth.

Also, in 2009 Liou et al.[10] used the reaction-sintering process $BiNbO_4$ doped with 0.5% of CuO obtaining 94% of the theoretical values in literature. And in 2010, Carneiro et al.[11] developed several prototypes comparing the results of the antennas on bismuth niobate ceramic substrates verifying that the high electrical permittivity of the material in the substrate reduces the dimensions of the antenna. Also, demonstrated the usage of the co-precipitation technique for the construction of the substrate by the starting materials: niobium pentoxide, bismuth nitrate, vanadium pentoxide and ammonium hydroxide.

Similarly, Sales et al.[12] analyzes bismuth niobate ceramics for applications in radio frequency (RF), however adding and modifying the copper concentration in the material proving to be a viable material for applications in this frequency range.

In addition, as microstrip antennas generally have low bandwidth and insufficient gain for such applications,

*e-mail: igormiranda@ufpa.br

periodic structures have been widely used in conjunction with $\varepsilon_r > 20$ substrates[13,14].

Oliveira et al.[13] uses the $BiNbO_4$ (V_2O_5) substrate with air holes as a periodic band gap (PBG) structure for the 10.26 GHz frequency band, finding good reflection coefficient (S_{11}) values, gain and bandwidth (B.W.) compared to others similar works. And Sousa et al.[14] simulated a microstrip antenna with graphene patch in terahertz band. They also used the PBG air holes structure to improve the results of the antenna.

And lastly also in 2020, Devesa et al.[15] described the dielectric properties of the $BiNbO_4$–$FeNbO_4$ ceramic at 2.8 GHz microwave band using the resonance cavity model, Furthermore, they used scanning electron microscopy and X ray diffraction to obtain the phase composition and morphology of the structure, thus enabling possible applications in microwave devices such as antennas, filters and others.

Therefore, in this work we use bismuth Niobate doped with vanadium oxide $BiNbO_4(V_2O_5)$, as the substrate of a miscrostrip antenna compared to a microstrip antenna of silicon dioxide SiO_2 both scaled to 5G at 3.5GHz. The simulations were carried out in the commercial software Ansys HFSS and CST Studio, to compare the results of the antennas we used the parameters reflection coefficient (S_{11}), bandwidth (BW), gain, radiation pattern (2D) and impedance Z_{11}. Moreover, we've made a brief comparison with other similar works in the literature.

1.1. Bismuth niobate

Bismuth niobate have been studied for applications in microwave and radio frequency range in the last decades. It's usually used for miniaturization devices due the high permittivity[4,5]. The most common method of preparation process of these oxides is the solid-state reaction, but, sometimes the Sol-gel method is used. Furthermore, the methods for measuring the dielectric properties vary from: Hakki-Coleman's, impedance spectroscopy, dielectric post (DP) resonator, and some variations of those. The references[6-13] obtained values of dielectric constant of 38 to 47 depending on the resonance frequency, τ_f, the addition of oxides and others.

For this work we used the coprecipitation process described in[11,12]. It consists of mixing, by heating the mixture at hot water bath, an amount of $Bi(NO_3)3.5H_2O$ dissolved in dilute HNO_3 also Nb_2O_5 and V_2O_5 dissolved in HF (hydrofluoric acid). After adding the vanadium for lowering the phase transition temperature and decrease the sintering temperature of $BiNbO_4$ ceramic, it was calcined at $T = 750°C$ and macerated. Finally, the ceramic is sintered at $T = 890°C$ and is ready. With this, the dielectric properties found were approximately: $\varepsilon_r = 47.8$, $tan\delta = 0.001$, Sintering temperature $T_s = 890°C$ and $Q > 1000$.

2. Antenna Project

The antenna was designed to operate at 3.5GHz frequency due to its applicability in the 5G band approved by the ITU. According to Balanis[16] the procedure below can be used to determine the dimensions for the antennas. First, by knowing the dielectric constant (ε_r) of the substrate and the resonance frequency (f_r) its calculated the patch width (Wp) by the Equation 1

$$W_p = \frac{1}{2 f_r \sqrt{\mu_0 \varepsilon_0}} \sqrt{\frac{2}{\varepsilon_r + 1}} \tag{1}$$

μ_0 and ε_0 are the magnectic permeability and electric permittivity in vacuum, respectively. Then, its calculated the effective dielectric constant (ε_{eff}), as function of W_p and the height of the substrate (h), by taking into account the edge effects and the speed of propagation of the field waves in the antenna given by the Equation 2.

$$\varepsilon_{eff} = \frac{\varepsilon_r + 1}{2} + \frac{\varepsilon_r - 1}{2} \sqrt{1 + \frac{12h}{W_p}} \tag{2}$$

After this, its calculated the normalized increment of the length ($\Delta l / h$) by Equation 3.

$$\frac{\Delta l}{h} = 0.412 \frac{(\varepsilon_{eff} + 0.3)\left(\frac{W_p}{h} + 0.264\right)}{\left(\varepsilon_{eff} + 0.258\right)\left(\frac{W_p}{h} + 0.8\right)} \tag{3}$$

Finally the real length of the patch (L_p) is calculated by Equation 4.

$$L_p = \frac{1}{2 f_r \sqrt{\varepsilon_{eff}} \sqrt{\mu_0 \varepsilon_0}} - 2\Delta l \tag{4}$$

So, using the Equations 1, 2, 3 and 4 it can be determined the length and the width of the patch. To determine the width of the line (W_f), the inset feed (f_i) and the gap (g) in the patch we use the procedure below. First we calculate the conductance by (5)

$$G_1 = \frac{-2 + \cos(X) - XS_{i(X)} + \frac{Sin(X)}{X}}{120\pi^2} \tag{5}$$

where, $X = \frac{2\pi W_f}{\lambda}$. Then we use Equation 6 to find G_{12} .

$$G_{12} = \frac{1}{120\pi^2} \int_0^{\pi} \left[\frac{\sin\left(k_0 W_f\right) 2\cos(\theta)}{\cos(\theta)} \right]^2 j_0\left(k_0 L_p sin\theta\right) sin^3(\theta) d\theta \tag{6}$$

where J_0 is the Bessel first kind zero order function. After this, we use Equation 7 to calculate the R_{in}

$$R_{in} = \frac{1}{2\left(G_1 + G_{12}\right)} \tag{7}$$

Finally, we determine the inset feed length by Equation 8.

$$f_i = \frac{L_p}{\pi} \operatorname{acos}\left(\sqrt{\frac{Z_{in}}{R_{in}}}\right) \tag{8}$$

and to determine the gap (g), we use the Equation 9.

$$g = \frac{3 \cdot 10^8 \times 4.65 \cdot 10^{-9}}{\sqrt{2 \times \varepsilon_{eff} \times f_r \times 10^{-9}}} \tag{9}$$

At last, it can be designed the antennas and finding the parameters disposed on Table 1, in which antenna 1 is with $BiNbO_4(V_2O_5)$ substrate and antenna 2 with SiO_2 substrate.

Table 1. Antenna parameters. Antenna 1 is the $BiNbO_4(V_2O_5)$ substrate and antenna 2 is the SiO_2 substrate.

Parameters	Antenna 1(mm)	Antenna 2(mm)
$W_{gp} \times L_{gp}$	20×25	60×55
$W_p \times L_p$	8.67617×4.5	27.1052×20.72
f_i	1.6	7
g	1	1.3
W_f	0.5	3
L	3	7
a	0.5	1.5
L_e	1.8	13
h	2.5	1.5

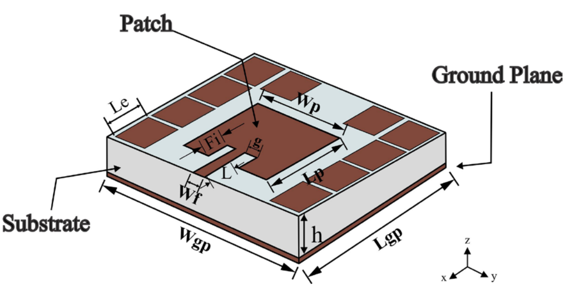

Figure 1. Antennas design with EBG structures.

The antennas design is common, differing only by the dimensions mentioned in Table 1. Figure 1 shows the antennas design.

2.1. Electromagnetic Band Gap (EBG)

Periodic structures have been used for a long time to improve the performance of microstrip antennas. Sievenpiper et al.[17] proposes the use of metallic structures characterized by High surface impedance creating a region where electromagnetic waves are prohibited at a certain frequency, depending on the periodicity. Because of that reduces the surface waves in the microstrip antenna patch and, consequently, increases its radiation efficiency and gain. These structures were initially proposed in photonic crystals, creating forbidden bands where light does not propagate. In antennas some structures are more usual like the mushroom structures[17,18].

In this case, the forbidden bands can be explained by a capacitive/inductive effect that happens due to the patches and pins that make up the structures.

One way to determine the band gap frequency for the structures is through an equivalent LC circuit[17,18]. The EBG structures vary according to the effect of the inductance (L) that connects the ground plane with the patches, these accumulate charge creating a capacitive effect (C). Thus, the Equation 10 determines the resonance frequency of the EBG structure.

$$\omega_0 = \frac{1}{\sqrt{LC}} \tag{10}$$

The inductance and capacitance can be calculated as a function of the pin (rod) radius (r), side size of the square EBG patch (Le) and distance between the patches center (s). Equations 11 and 12 calculate L and C, respectively.

$$L = 2\times 10^{-7} h\left[\ln\left(\frac{2h}{r}\right) + 0.5\left(\frac{2r}{h}\right) - 0.75\right] \tag{11}$$

$$C = \frac{L_e \varepsilon_0 \left(1+\varepsilon_r\right)}{\pi}\cosh^{-1}\left[\frac{L_e + s}{s}\right] \tag{12}$$

So, in this paper we calculated the resonance frequency of the copper periodic structure (EBG), as shown in Figure 1, according to the Equations 10, 11 and 12. This is equivalent to a LC circuit like if the EBG patches act as capacitors plates and the rods as inductors[17,18].

3. Results and Discussions

In this work we use the Finite Elements Method (FEM) and Finite Integral Technique (FIT) simulating in the commercial software ANSYS HFSS and CST Studio Suite 2019, respectively.

The FEM is a method for solving related equations by approximating the continuous field variables at discrete points (nodes), such that the more points are used the better is the solution. In Ansys HFSS, the FEM divides the antenna geometry into small pieces (mesh) and for each of them, calculates the Electric Field ($\vec{E}$) in the mesh nodes. This way, it can determine the $\vec{E}$ in all space associating with the appropriated boundary conditions. So, the time dependent Maxwell's equations used in Ansys HFSS are (13) and (14) depending on the problem.

$$\nabla \times \vec{E} = -\frac{\partial \vec{B}}{\partial t} \tag{13}$$

$$\nabla \times \vec{H} = \vec{J} + \frac{\partial \vec{D}}{\partial t} \tag{14}$$

Where $\vec{E}$ is the electric field, $\vec{H}$ is the magnetic field, $\vec{D}$ is the electric flux density and is the magnetic flux density. Also the constitutive relations are $\vec{D} = \varepsilon \vec{E}$ and $\vec{B} = \mu \vec{H}$.

In CST Studio the FIT discretizes the geometry in tetrahedral meshes and uses the integral Maxwell's Equations 15 and 16.

$$\int_c \vec{E}\cdot d\vec{l} = -\int_A \frac{\partial \vec{B}}{\partial t}\cdot d\vec{A} \tag{15}$$

$$\int_c \vec{H}\cdot d\vec{l} = \int_A \left(\vec{J} + \frac{\partial \vec{D}}{\partial t}\right)\cdot d\vec{A} \tag{16}$$

In this case, it generates the Maxwell's equations in a discrete form called Maxwell's Grid Equations, using matrices, i.e., Maxwell's equations and the related material equations are changed from the continuous to the discrete space by allocating electric voltages on the edges and electric fluxes on the faces of a grid and magnetic voltages on the edges and magnetic fluxes on the faces of a second grid, it summarizes the method.

Thus, Figure 2 shows the S_{11} of each antenna in dB. We can see that the antenna 2 obtained 100MHz bandwidth and around -30dB of S_{11} values at 3.5 GHz. On the other hand, antenna 1 obtained two resonances at approximately 3.5GHz and 4.1GHz. The first resonance has 80 MHz of bandwidth and -20dB of reflection coefficient. The second resonance has 50MHz of bandwidth and -17dB of reflection coefficient. We notice that the values of bandwidth are lower than the antenna 2 results, but still a great option due the advantages of weight and size of antenna 1.

In addition, it is important to check the match of the line with the patch through the impedance graph (Z_{in}) where the real part Z_{in}(Re) represents the input resistance values of the antennas and the imaginary impedance values Z_{in}(Im) represents the input reactance of the antennas. Figures 3a and 3b show the resistance and reactance values in Ohms(Ω). The closer the real impedance part value is to 50 Ω the better and the closer the imaginary part is to zero, too.

Antenna 1 obtained values of 56 Ω and 60 Ω of resistance on softwares Ansys HFSS and CST Studio, respectively. The reactance was 5.2Ω and 1.4Ω in the Ansys HFSS and CST Studio software, respectively. Antenna 2 obtained the values of 45.1Ω and 48Ω of resistance, and -2.4Ω and 1.01Ω of reactance on softwares Ansys HFSS and CST Studio, respectively.

Besides, it is possible to check the radiation Diagram (2D) in Figure 4a, b, c and d obtained to the antennas in Ansys HFSS and CST Studio. Note that antenna 1 has good values compared to antenna 2 even with the reduction of its volume.

The Table 2 shows the results for both softwares and compare to others works with similar proposal. It's analyzed the values of S_{11}, resonance frequency(GHz), gain (dB), bandwidth (B.W.), periodic structures, substrate material and the ε_r value.

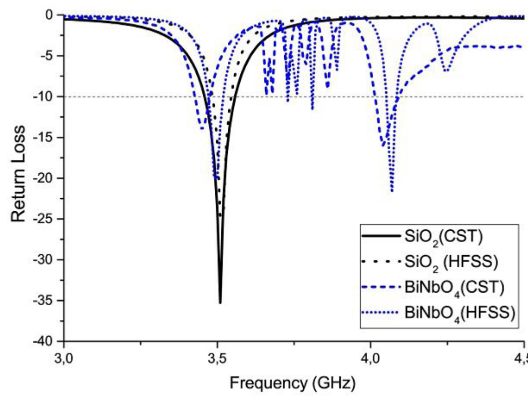

Figure 2. Antennas in black are simulated on CST Studio and Ansys HFSS with SiO_2 substrate and in blue are simulated in CST Studio and Ansys HFSS with $BiNbO_4$ substrate.

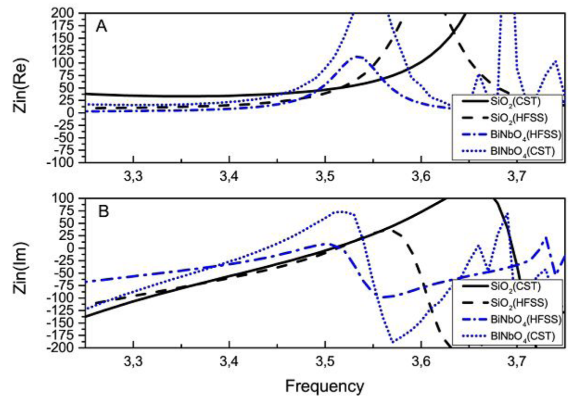

Figure 3. (a) shows the resistance of the antennas, in black and in blue the SiO_2 and $BiNbO_4$ antennas, respectively, simulated in CST and HFSS. (b) shows the reactance of the antennas, in black and in blue the SiO_2 and $BiNbO_4$ antennas, respectively, simulated in CST and HFSS.

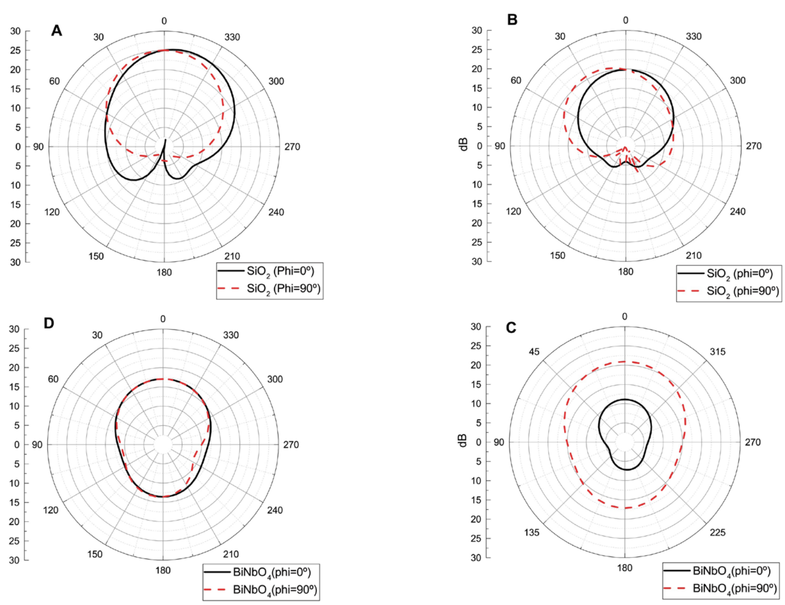

Figure 4. (A), (B), (C) and (D) shows the Radiation Diagram (2D) of the antennas 1 and 2 simulated in Ansys HFSS and CST Studio softwares. In A, Antenna 2 simulated in Ansys HFSS, in B, Antenna 2 simulated in CST Studio, in C, Antenna 1 simulated in Ansys HFSS and D Antenna 1 simulated in CST Studio.

Table 2. Comparison of S_{11}, gain, B.W., use of periodic structures, substrate material and ε_r parameters, of recently papers that use high permittivity materials in microvawe aplications, with ours results.

Paper	S_{11}(Res.Freq.)	Gain(dB)	B.W.(MHz)	Per.Struc.	Material	ε_r
Zhou et al.[9]	-22.0 (3.07GHz)	-	34	-	$BiNbO_4(V_2O_5)$	43
Carneiro et al.[11]	-11.4 (2.64GHz)	-	100	-	$BiNbO_4(V_2O_5)$	47,8
Sales et al.[12]	-40 (12.5GHz)	4.4	200	-	$BiNbO_4$	47
Liu et al.[19]	-22(5GHz)	-	280	FSS	FR4	4.4
Kulkarni and Sharma[20]	-24 and -32(1.8 – 2.6GHz)	3 and 5	100 - 80	-	FR4	4.4
Proposed (SiO_2)	-24.7 (3.51GHz)	7.7	100	EBG	SiO_2	4
Proposed ($BiNbO_4$)	-20 (3.5GHz)	3.6	80	EBG	$BiNbO_4(V_2O_5)$	47.4

At this frequency band, the S_{11} results of the antenna 1 disposed above are excellent when compared to the shown works. Liu et al.[19] prototyped a microstrip antenna with FR4 substrate ($\varepsilon_r = 4.4$) and frequency selective surfaces (FSS) at the ground plane, aiming to reduce the antenna dimensions. The results of S_{11} (-22 at 5GHz) and approximately 280 MHz of bandwidth are excellent, the paper does not present the gain results. If comparing with antenna 2, we notice a similar result of antenna 2 but with less volume, due the FSS applied. But, antenna 1 has got better results than the reference in gain and volume reduction presented in the paper.

Kulkarni and Sharma[20] designed a reconfigurable microstrip loop antenna multiband with MIMO application. This antenna is designed to operate in 3 bands with FR4 substrate, the best results are -24 dB and -32 dB at 1.8GHz and 2.6GHz respectively, 3dB and 5dB of gain and 100MHz of bandwidth. The antenna is extremely bigger than antennas 1 and 2 and it's visible that the EBG structures can enhance the gain parameter of the antennas, if comparing it with our designed antennas. So, with this it can be shown that the use of EBG structures can provide great enhancement in gain results, as well as the use of high dielectric materials provide volume reduction and bandwidth improvement.

As well as the gain and bandwidth results when compared to the antennas of[9,11,12], due to the considerable volume reduction. This way, in comparison with the most recently works using the same substrate material[9,11-13] the $BiNbO_4$ with addition of V_2O_5 antenna can be a good option for application at S Band and 5G communications technologies.

4. Conclusions

Two antennas with EBG structures were designed and compared using the software Ansys HFSS and CST Studio to operate at S band (3.5 GHz) 5G technology. The results demonstrate that the proposed $BiNbO_4$ antenna has great advantage in relation to those mentioned in terms of volume reduction, presenting results similar to those antennas with higher volume. So, it's visible that the EBG structures have provided great improvement of gain, due its surface waves reduction on the patch. Also, the $BiNbO_4$ substrate material leads to a considerable reduction in the total volume of the antenna. This way, the proposed Bismuth Niobate antenna proves to be an excellent alternative for microwave devices, highlighting the mentioned advantages.

5. References

1. Liu G, Jiang D. 5G: Vision and requirements for mobile communication system towards year 2020. Chin J Eng. 2016;2016:1-8.
2. Henry S, Alsohaily A, Sousa ES. 5G is real: evaluating the compliance of the 3GPP 5G new radio system with the ITU IMT-2020 requirements. IEEE Access. 2020;8:42828-40.
3. Sebastian MT, Jantunen H, Ubic R, editors. Microwave materials and applications. Hoboken: John Wiley & Sons; 2017. p. 349-54.
4. Fujimoto K, Morishita H. Modern small antennas. Cambridge: Cambridge University Press; 2013. p. 266-63. (vol. 2).
5. Pandey S, Kumar D, Parkash O, Pandey L. Design and Development of dielectric resonator antenna using ceramic materials: an overview. Trans Indian Inst Met. 2019;72(8):2019-28.
6. Yang C-F. Improvement of the dielectric properties of $BiNbO_4$ ceramics by the addition of CuO-V_2O_5 mixtures. J Mater Sci Lett. 1999;18(10):805-7.
7. Tzou W-C, Yang C-F, Chen Y-C, Cheng P-S. Improvements in the sintering and microwave properties of $BiNbO_4$ microwave ceramics by V_2O_5 addition. J Eur Ceram Soc. 2000;20(7):991-6.
8. Shihua D, Xi Y, Yong Y. Dielectric properties of B_2O_3-doped $BiNbO_4$ ceramics. Ceram Int. 2004;30(7):1195-8.
9. Zhou D, Wang H, Jiang Y, Yao X. The two element antennas using $BiNbO_4$ ceramics as the substrate. Mater Sci Eng A. 2007;460-461:652-5.
10. Liou Y-C, Tsai W-C, Chen H-M. Low-temperature synthesis of $BiNbO_4$ ceramics using reaction-sintering process. Ceram Int. 2009;35(6):2119-22.
11. Carneiro R Fo, Araújo JH, Ginani MF, d'Assunção AG Jr, Martins RA, d'Assunção AG, et al. Simulation and measurement of inset-fed microstrip patch antennas on BiNbO4 substrates. Microw Opt Technol Lett. 2010;52(5):1034-6.
12. Sales AJM, Oliveira PWS, Almeida JS, Costa MM, Rodrigues HO, Sombra ASB. Copper concentration effect in the dielectric properties of BiNbO4 for RF applications. J Alloys Compd. 2012;542:264-70.
13. Oliveira JE, Sousa FM, Sousa FB, Oliveira OTB, Paschoal W, Costa MBC. Microstrip antenna on $BiNbO_4$:V2O_5 substrate with electromagnetic bandgap/photonic bandgap array. J Comput Theor Nanosci. 2018;15(11):3088-92.
14. Sousa FM, Sousa FB, Miranda IRS, Oliveira JE, Paschoal W Jr, Costa MBC. Graphene patch antenna with lateral edges defined by armchair or zigzag structures and PBG substrate. J Comput Electron. 2020;19(2):700-8.
15. Devesa S, Graça MP, Costa LC. Microwave Dielectric Properties of the Binary System $BiNbO_4$–$FeNbO_4$. ECS J Solid State Sci Technol. 2020;9(9):093010.
16. Balanis CA. Antenna theory: analysis and design. 4th ed. Hoboken: John Wiley & Sons, 2016. p. 783-867.

17. Sievenpiper D, Lijun Zhang, Broas RFJ, Alexopolous NG, Yablonovitch E. High-impedance electromagnetic surfaces with a forbidden frequency band. IEEE Trans Microw Theory Tech. 1999;47(11):2059-74.
18. Joannopoulos JD, Johnson SG, Winn JN, Meade RD. Photonic crystals: molding the flow of light. Princeton: Princeton University Press; 2011.
19. Liu Y, Hao Y, Wang H, Li K, Gong S. Low RCS microstrip patch antenna using frequency-selective surface and microstrip resonator. IEEE Antennas Wirel Propag Lett. 2015;14:1290-3.
20. Kulkarni AN, Sharma SK. Frequency reconfigurable microstrip loop antenna covering LTE bands with MIMO implementation and wideband microstrip slot antenna all for portable wireless DTV media player. IEEE Trans Antenn Propag. 2013;61(2):964-8.